



## Raman Microscopy as a Tool for the Rust Composition Distribution Analysis

### Microscopía Raman como Herramienta para el Análisis de Distribución de la Composición de Herrumbres

F. R. Pérez<sup>\*a</sup>, C. A. Barrero<sup>b</sup>, K. García<sup>b</sup>, A. H. High Walker<sup>c</sup>

<sup>a</sup> Grupo de Óptica y Espectroscopia (GOE), Universidad Pontificia Bolivariana, Cq. 1 #70-01, Medellín, Colombia.

<sup>b</sup> Grupo de Estado Sólido, Sede de Investigaciones Universitaria, Universidad de Antioquia, A. A. 1226, Medellín, Colombia.

<sup>c</sup> Physics Laboratory, National Institute of Standards and Technology, (NIST), Gaithersburg, MD 20899, USA.

Recibido 01.03.10; Aceptado 05.11.10; Publicado en línea 17.01.11.

#### Resumen

Una adecuada identificación de los diferentes componentes presentes en productos de corrosión de aceros es una tarea que normalmente requiere la utilización de diferentes técnicas analíticas. Las técnicas clásicas que los científicos de la corrosión han usado para la realización tanto de estudios cualitativos como cuantitativos son la espectroscopia Mossbauer y la difracción de rayos X. Recientemente algunas otras técnicas han ganado importancia en este campo. Una de estas técnicas es la microscopía Raman. En este trabajo se obtuvieron espectros de microscopía Raman de herrumbres. Se realizó un barrido a lo largo de una línea recta de 100  $\mu\text{m}$  de longitud mediante pasos de 10  $\mu\text{m}$ . Se identificaron bandas características de magnetita, lepidocrocite, goetita y akaganeita, las cuales mostraron diferentes intensidades relativas en cada punto. Las intensidades relativas de las bandas más representativas de cada fase se usaron para asignar factores de peso que se usaron para la cuantificación de cada fase de hierro para intentar la determinación de la composición de la capa superficial de herrumbre. Así, se intenta proponer un método cuantitativo para la determinación de la distribución de fases en la capa de herrumbre.

**Palabras clave:** Microscopía Raman, Corrosión y protección.

#### Abstract

The proper identification of different components contained in steel corrosion products is a task which normally requires the use of different analytical techniques. Mössbauer spectrometry and X-ray diffraction have been the classical techniques used by corrosion scientists to carry out both qualitative and quantitative studies. Recently other techniques have been widely used in qualitative studies of rusts: one of these techniques is Raman microscopy. In this work, Raman microscopy spectra of rust were obtained. Scanning across a 100  $\mu\text{m}$  length straight line was obtained by a pass of 10  $\mu\text{m}$ . Characteristic bands of magnetite, lepidocrocite, goethite and akaganeite were identified showing different relative intensities on each point. The relative intensities of the mayor bands of each phase were used for assigning weight factors which were used for the quantification of each iron phase to try to determine the rust layer composition. In this way, a quantitative method for the phase composition determination of the rust layer was proposed.

**Keywords:** Raman microscopy, Corrosion protection.

**PACS:** 78.30.-j, 81.65.Kn.

© 2010 Revista Colombiana de Física. Todos los derechos reservados.

\* fredy.perez@upb.edu.co

## 1. Introduction

Raman microscopy is the application of Raman spectroscopy to the study of small samples. Because a typical Raman spectrum of a micro-metric size sample can be of the order of 1012 times smaller than that for Rayleigh scattering, the use of this technique was not usable before the introduction of an efficient method for rejecting the latter. This was possible by the introduction of notch filters. In addition, the use of enhanced charge coupled devices (enhanced CCD) allowed the creation of more suitable systems for the multichannel detection method. A modern Raman microscopic system combines the advantages coming from a confocal architecture, the optimized design of the spectrometers, the laser technology advances, the CCD detection, the holographic notch filters technology and the computer control to obtain a powerful machine used in materials characterization [1]. The application of Raman microscopy in the iron oxides and oxy-hydroxides characterization probably started with the classic work by De Faria et al. [2]. One of the most cited works related to Raman microscopy on steel corrosion products has been the Cook's et al. one [3]. Neff et al. [4] have used this technique in the characterization of iron archaeological artefacts. However, most papers found in literature include qualitative analysis only identifying the phases present in the corrosion products. Dubois et al. [5] have recently proposed a method based on Raman mapping for the characterization of steel corrosion products determining their respective mass fraction. However, their method requires the obtention of spectra of different iron oxides and oxy-hydroxides mixed in different proportions. In this work, we propose a new method for the phase identification and the relative abundance determination of the rust components, by using the relative intensity and the mean height width (MHW) of some characteristic Raman bands of the iron phases present in the rusts.

## 2. Experimental Methods

Details on the rusts obtention procedure can be found in our previous papers [6,7]. The Raman microscopy spectra of pellets made from powder were measured using an InVia Renishaw Ramanscope system. The sample translation system allows XY displacements with a 1  $\mu\text{m}$  step and the scanning can be done across straight lines, squares and circumferences. The measurements were carried out in air using the He-Ne excitation line of 633 nm. The power of the laser source was 25 mW. However, this power was attenuated to the minimum value allowed by the instrument, in such a way that the measured laser power on the sample was about 0.24 mW. Structural transformations of the iron phases due to the laser action were not expected because these transformations can occur when the power on the sample is higher than 0.7 mW [2].

However, the temperature on the sample was evaluated using the method by Pérez et al. [6] and its value was about 100  $^{\circ}\text{C}$ , which is below the temperature required for thermal transformations of iron oxides and oxy-hydroxides. All spectra were taken using a 50X microscope objective and an integration time of 60s. The spectral window was between 100 and 800  $\text{cm}^{-1}$  corresponding to the region in which the iron phases detected in this study have their major phonon lattice modes [3, 4]. Scanning across a straight line of 100  $\mu\text{m}$  length was obtained. The scanned points are on the X-coordinate axis and their coordinates are (-50  $\mu\text{m}$ , 0), ..., (50  $\mu\text{m}$ , 0) (see Fig. 2 down-right). Hence, eleven different spectra were taken. Those spectra are shown in Fig. 1 and 2, and they have been labelled as E1, E2, ..., E11. It is important to clarify that the coordinates of E1, E2, ..., E11, are (-50  $\mu\text{m}$ , 0), (-40  $\mu\text{m}$ , 0), ..., (50  $\mu\text{m}$ , 0), respectively. All the spectra were fitted by the WIRE 2.0 program accompanying the system, and using voigtian curves.

## 3. Results and Discussion

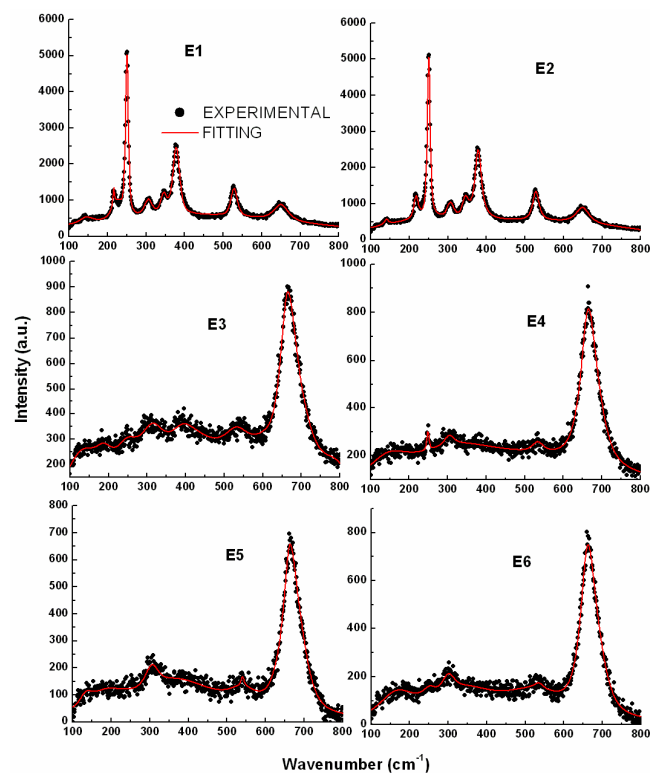


Fig. 1: Raman spectra measured at points E1 to E6.

For a proper identification of each iron phase by Raman spectroscopy, we have taken into consideration the most important bands reported for each iron phase as follows [2, 3, 4]: for  $\gamma$ -FeOOH the bands located at 219,

252 and 650  $\text{cm}^{-1}$  were used; for goethite the bands used were at 300 and at 386  $\text{cm}^{-1}$ ; the bands at 314 and 722  $\text{cm}^{-1}$  were used for identifying  $\beta$ -FeOOH; finally, for Fe<sub>3</sub>-xO<sub>4</sub> the bands at 532 and at 667  $\text{cm}^{-1}$  were used. The band located at about 380  $\text{cm}^{-1}$  cannot be used as a criterion for identification of any phase, because it is a superposition of the strongest bands of goethite and  $\beta$ -FeOOH, and also to the next strongest bands of  $\gamma$ -FeOOH.

The composition of our rusts was extensively discussed in our previous works [6, 7]. Non-stoichiometric magnetite (Fe<sub>3</sub>-xO<sub>4</sub>), magnetic and super-paramagnetic goethite ( $\alpha$ -FeOOH), ledebrockite ( $\gamma$ -FeOOH) and akaganeite ( $\beta$ -FeOOH) were the iron phases detected. All the spectra showed characteristic bands of most of them, but the relative intensities and widths resulted different in all cases, indicating different relative abundances in different regions of the sample. The band intensities can be seen in Fig. 1 and 2, in which the experimental data (full circles) and the respective fitting curves are shown. After the fitting processes, the maximum and the MHW values of each band were measured. The summation of the product of these two parameters for the bands associated to each phase was taken as a measurement of their abundances,  $A_i$ . Now, if we consider the total area under the fitting curve as being proportional to the total mass in the illuminated area,  $A$ , the quotient between  $A_i$  and  $A$  can be taken as a measurement of the relative mass fraction phase (or relative abundance), and  $(A_i / A) \times 100$  as the respective percent relative phase abundances. In Table No. 1, the relative abundances (% Mass) estimated as explained before for each scanned point are presented, as well as the average values taken over the total data for each iron phase. In addition, in the last column, the respective relative abundances as calculated by Rietveld refinement [8] are presented. All values are different which can in part be explained in the following way: a Raman spectrum from a sample consisting of a mixture of iron oxides and oxy-hydroxides presents superposition of various bands making proper band assignment too difficult. On the other hand, some kind of super-paramagnetic phases can not be detected by X-ray diffraction measurement ( $\gamma$ -Fe<sub>2</sub>O<sub>3</sub> and  $\alpha$ -FeOOH), but Raman microscopy could detect them finding different values in all relative abundances. However, our method would be enhanced and used as a powerful tool for the phase relative quantification of products of steel corrosion, if the statistics were better, i. e., if a higher number of points was scanned and mapped. This implies that a more representative sampling is taken into account in the scanning process.

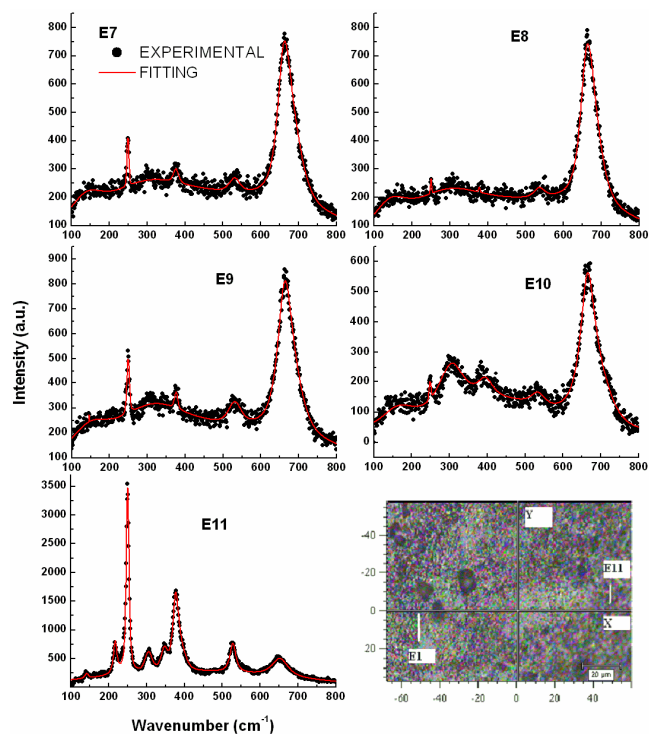


Fig. 2: Raman spectra measured at points E7 to E11. Optical microscopy image of the scanned region (Down-right).

As it is well known, the XDR lateral resolution is of the order of mm whereas its depth resolution can vary between 20 Å to 30  $\mu\text{m}$ , depending on the materials' properties and x-ray incidence angle. In relation to Raman microscopy, both lateral resolution and confocal mode depth resolution are of the order of  $\mu\text{m}$ . In this way, a smaller area is studied by Raman microscopy which is an indicative of its better resolution compared with that of XRD. Because a more localized analysis is obtained by Raman microscopy, it is possible to have a more precise measurement of the composition of the sample.

#### 4. Conclusions

A method for the determination of relative abundances of iron oxides and oxy-hydroxides present in rusts was presented. The method is based on Raman mapping. The most representative Raman bands associated to each phase were employed. The method would be enhanced if a higher number of points was used in the scanning process which means a more representative mapping in the measured region of the sample.

Table No. 1: Relative abundances (% Mass) of iron phases detected in rusts, their average (Av.) and their respective values obtained by Rietvel refinement (Riet.).

Relative Abundance (% Mass)	E1	E2	E3	E4	E5	E6	E7	E8	E9	E10	E11	Av.	Riet.
$\beta$ -FeOOH	7	3	51	56	9	69	59	60	56	32	6	37	31
$\alpha$ -FeOOH	26	28	6	4	51	0	2	0	2	9	28	14	24
$\gamma$ -FeOOH	53	59	23	23	0	4	7	1	12	3	66	23	10
Fe <sub>3</sub> -xO <sub>4</sub>	14	10	19	17	40	27	32	39	30	56	0	26	35

### 5. Acknowledgments:

Thanks go to Universidad de Antioquia (project code IN1248CE, Sustainability Programs for GES) and Universidad Pontificia Bolivariana (project code 889-05/06-27), and the Excellence Center for Novel Materials (CENM) under Contract CENM - Colciencias RC-043-2005 for financial support.

### References

[1] Baldwin, K. J. Raman Microscopy: Confocal and Scanning Near-Field. In: Lewis, I. R. et al. Handbook of Raman Spectroscopy. New York: Marcel Derker, Inc., 2001. p. 145-190.

[2] D.L.A. de Faria, V. Silva, M.T. de Oliveira, Raman microspectroscopy of some iron oxides and oxy-hydroxides, *J. Raman Spectrosc.* 28 (1997) 873.

[3] S.J. Oh, D.C. Cook, T.E. Townsend, Characterization of Iron Oxides Commonly Formed as Corrosion Products on Steel, *Hyp. Interact.* 112 (1998) 59.

[4] D. Neff, L. Bellot-Gurlet, P. Dillmann, S. Regeur, L. Legrand, Raman imaging of ancient rust scales on archaeological iron artefacts for long-term atmospheric

corrosion mechanisms study, *J. Raman Spectrosc.* 37 (2006) 1228.

[5] F. Dubois, C. Mendibide, T. Pagnier, F. Perrard, C. Duret, Raman mapping of corrosion products formed onto spring steels during salt spray experiments. A correlation between the scale composition and the corrosion resistance, *Corrosion Science* 50 (2008) 3401–3409.

[6] F.R. Pérez, C.A. Barrero, O. Arnache, L.C. Sánchez, K.E. García, A.R. Hight Walker, Structural properties of iron phases formed on low alloy steels immersed in sodium chloride-rich solutions, *Physica B: Condensed Matter*, 404 (2009) 1347–1353.

[7] F.R. Pérez, C.A. Barrero, A.R. Hight Walker, K.E. García, K. Nomura, Effects of chloride concentration, immersion time and steel composition on the spinel phase formation, *Materials Chemistry and Physics* 117 (2009) 214–223.

[8] F. R. Pérez. Corrosion Of Steels In Total Immersion Tests: Characterization of Products and Discussion of the Dynamical Processes, Medellín-Colombia, 2009, pag. 93-94. Ph. D. Thesis. Universidad de Antioquia. Facultad de Ciencias Exactas y Naturales. Posgrado en Física.